






## Chrome(VI) ion biosorption modelling in a fixed bed column on *Dioscorea rotundata* hull

Angel Villabona-Ortíz<sup>1</sup> , Candelaria Tejada-Tovar<sup>1</sup> , Rodrigo Ortega Toro<sup>2</sup>  ,  
Keily Peña-Romero<sup>1</sup> , Ciro Botello-Urbiñez<sup>1</sup>

<sup>1</sup> Universidad de Cartagena, Department of Chemical Engineering, Cartagena de Indias, Colombia

<sup>2</sup> Universidad de Cartagena, Department of Food Engineering, Av. del Consulado # 30 St., No. 48 152 Cartagena, Cartagena de Indias, Bolívar Cartagena de Indias, Colombia

RECEIVED 09.11.2020

ACCEPTED 26.08.2021

AVAILABLE ONLINE 29.06.2022

**Abstract:** This work aimed to evaluate the yam peel in a bed column packaged as a chromium(VI) ion adsorbent in an aqueous solution. Yam peel was used as adsorbent, prior washing, drying, size reduction, and selection. The experimental work consisted in determining the effect of bed depth, particle size, and temperature, keeping inlet flow =  $0.75 \text{ cm}^3 \cdot \text{s}^{-1}$ , pH = 2 and initial concentration of  $100 \text{ mg} \cdot \text{dm}^{-3}$ . The Adsorption Scanning Electron Microscopy (SEM) and Energy Dispersive X-ray (EDS) analysis on yam (*Dioscorea rotundata*) peel showed a heterogeneous, porous structure, with functional groups characteristic in lignocellulosic materials. It was analysed regarding the influence of temperature, bed height, and adsorbent particle size on the removal efficiency; it was found that the decrease of particle size and the increase of the bed height favour the elimination of the metallic ion, with removal rates between 92.4 and 98.3%. The bed maximum adsorption capacity was  $61.75 \text{ mg} \cdot \text{g}^{-1}$ , and break time of 360 min. The break curve's adjustment to the Thomas, Yoon–Nelson, Dose–Response and Adams–Bohart models was evaluated, concluding that the Yoon–Nelson and Dose–Response models best described the behaviour of the break curve with a coefficient of determination ( $R^2$ ) of 0.95 and 0.96, respectively. The results show that the bio-adsorbent studied can be used to eliminate Cr(VI) in a continuous system.

**Keywords:** adsorbent, adsorption, Dose–Response model, Yoon–Nelson model

### INTRODUCTION

Chromium (Cr) compounds are among the most common environmental pollutants due to their extensive industrial applications [CHINYELU *et al.* 2018]. The trivalent [Cr(III)] and hexavalent [Cr(VI)] oxidation states of chromium are the most stable and abundant in the natural environment; however, they differ significantly in their physicochemical properties, bioavailability, and toxicity to living organisms [SUKUMAR *et al.* 2017].

Hexavalent chromium [Cr(VI)] is one of the most harmful heavy metals and is the third most common pollutant in hazardous waste effluents, and is the most carcinogenic substance [ARANDA-GARCÍA, CRISTIANI-URBINA 2020]. In addition, Cr(VI) is highly soluble in water, movable in aqueous systems, and toxic, causing severe physiological and neurological effects on

human and animal health, such as anaemia, diarrhoea, nausea, epigastric pain, ulcers, vomiting, eye and skin irritation, injury to nerve tissues, kidney and liver, lung congestion, internal bleeding, and circulatory system failure [SRIVASTAVA *et al.* 2019]. It is also highly mutagenic, as it can induce DNA damage and congenital disabilities, affect gene expression, and reduce reproductive health [ACHMAD *et al.* 2017]. Furthermore, Cr(VI) is toxic to plants since it seriously affects several biochemical processes, physiological and morphological, leading to slow growth, chlorosis, and necrosis.

Therefore, removing Cr(VI) from industrial effluents is important before discharge to aquatic environments or land. Biosorption is presented as an effective alternative to remove Cr(VI) from wastewater [MARTÍN-LARA *et al.* 2017]. Thus, various conventional physical, chemical, and biological technologies have

been implemented to remediate Cr(VI) contaminated wastewater and contaminated water, and avoid or reduce its adverse effects on human health and the environment [PARLAYICI, PEHLIVAN 2019]. These include reverse osmosis, ion exchange, oxidation, photocatalysis, heterogeneous catalysis, and ultrafiltration [BHANVASE *et al.* 2017]. However, in many cases, these are inconvenient due to their low efficiency at low concentrations, costs of raw materials and energy consumption, generation of toxic by-products, and the difficulties in their handling and treatment limit the use of conventional methods in industrial applications [BHANVASE *et al.* 2017].

Biosorption has been considered a promising and attractive technology to remove Cr(VI) from polluted waters in an efficient, competitive, economic, and ecological way [SAHU, SINGH 2019]. Some of the advantages of biosorption are low cost, high efficiency, minimisation of chemical and biological sludge, no need for additional nutrients, regeneration of biosorbents, and the possibility of metal recovery [SUKUMAR *et al.* 2017]. However, most of the research on Cr(VI) removal by bio-adsorption has been done in batch systems because they can be applied with effortless ease on a laboratory scale but challenging to use on a large scale, mainly when the volume of industrial effluent requiring treatment is large [ELABBAS *et al.* 2016]. In addition, data from batch systems may not apply to continuous fixed-bed column operations, where the contact time is not long enough to reach equilibrium [CHERDCHOO *et al.* 2019]. Therefore, it is crucial to determine the practical applicability of a biosorbent in the continuous operation mode [BHARATHI, RAMESH 2013]. However, in large-scale processes, fixed-bed column systems are preferred because of their high effectiveness, simplicity of operation, low cost, and ability to be expanded from a laboratory process to produce higher quality effluent [JAFARI, JAMALI 2016].

Agricultural residues are commonly used as heavy metal adsorbents because they are mainly composed of proteins, polysaccharides, and lignin [RONDA *et al.* 2015]. Since very little information is found in the literature on bio-adsorption scaling, the objective of this work was to evaluate the effects of different parameters (temperature, bed height, and particle size) on the removal of Cr(VI) by yam shells in a continuous bed system.

## MATERIALS AND METHODS

### MATERIALS AND REAGENTS

All the chemicals and reagents used in this work were of analytical reactive grade. Potassium dichromate ( $K_2Cr_2O_7$ ) was used to prepare the chrome solution at  $100 \text{ mg}\cdot\text{dm}^{-3}$ . HCl and NaOH 1 M were used to adjust the pH of the solution.

The yam (*Dioscorea rotundata*) peel was obtained as a by-product of post-harvest handling. The biomass with the best condition was selected to guarantee its lignocellulosic nature, and washed with deionised water, and dried in a Lauda Alpha oven at  $60^\circ\text{C}$  for 24 hours. Size reduction was made in a roller mill; size classification was made in an Edibon Orto Alesa shaker type sieve using stainless steel sieves of mesh sizes 100, 45, 35, 18, and 16, to select particle sizes proposed in the design of experiments. The bio-adsorbent was examined by Scanning Electronic Micro-

scopy (SEM) and Energy Dispersive Spectrometry (EDS) to study its morphology and elemental composition before and after the adsorption [BIBAJ *et al.* 2019].

## METHODS

### EXPERIMENTAL DESIGN

The adsorption tests in a continuous system were carried out following a design of experiments with a continuous linear factor in response surface of the central compound. The study used Statgraphics Centurion XVI.II. This type of design of experiments allows to analyse the effect variables produce when varying them simultaneously on the dependent variable. The study involved a limited number of experiments without the need for replicas, and response surface mapping [DEMIREL, KAYAN 2012]. Particle size, adsorbent dose, and temperature were varied for a total of 16 experiments per bio-adsorbent. Table 1 summarises the range and levels of variation implemented.

**Table 1.** Ranges and levels of variation

Independent variable	Range and level				
	$-\alpha$	-1	0	+1	$+\alpha$
Particle size (mm)	0.13	0.355	0.6775	1	1.22
Bed height (mm)	6.13	30	65	100	123.8
Temperature ( $^\circ\text{C}$ )	29.8	40	55	70	80.22

Explanations:  $-\alpha$  and  $+\alpha$  = values below and over the range provided by Statgraphics Centurios, respectively, -1 and +1 = the lowest and higher value supplied to the software during experimental design, and 0 is the centre point.

Source: own study.

### COLUMN ADSORPTION TESTS

The synthetic solution of Cr(VI) was prepared by adding  $0.283 \text{ g } K_2Cr_2O_7$  per  $\text{dm}^3$  of deionised water for a concentration of  $100 \text{ mg}\cdot\text{dm}^{-3}$ . Adsorption tests were performed in equipment with acrylic columns in which the solution flowed by the action of gravity with a flow rate of  $0.75 \text{ cm}^3\cdot\text{s}^{-1}$  at pH 2. The concentration of Cr(VI) was determined by taking a sample at the exit of the column; a UV-VIS spectrophotometer was used at 540 nm, Biobase brand, using 1.5 diphenyl carbazide indicator, according to ASTM D1687-17 [SUKUMAR *et al.* 2017]. Adsorption efficiency (AE, in %) was determined by Equation (1):

$$AE = \frac{C_0 - C_i}{C_0} 100 \quad (1)$$

where:  $C_0$  = initial concentration of the test metal and  $C_i$  = concentration of the test metal after the adsorption process [ABDOLALI *et al.* 2017].

The Statgraphics Centurion software was used to study the effect of temperature, particle size, and bed height through analysis of variance and effect diagrams to establish the statistical significance of the evaluated variables on removal efficiency.

## MODELLING OF THE BREAKAGE CURVE

The modelling of the break curve was done at the best experimental condition found, and the data obtained fit the Adams–Bohart, Thomas, Yoon–Nelson, and Dose–Response models, summarised in Table 2. These models allow the analysis of Cr(VI)'s dynamic adsorption rate, bed service time, and process breakage time [RODRIGUES *et al.* 2019]. The adjustment of the models was established according to the correlation coefficient ( $R^2$ ).

**Table 2.** Adjustment models for the rupture curve

Model	Equation	Parameter explanation
Adams–Bohart (AB)	$\frac{C}{C_0} = \frac{\exp(K_{AB}C_0t)}{\exp\left(\frac{K_{AB}N_0L}{v}\right) - 1 + \exp(K_{AB}C_0t)}$	$K_{AB}$ = model constant ( $\text{dm}^3\cdot\text{mg}^{-1}\cdot\text{min}^{-1}$ ) $N_0$ = maximum volumetric adsorption capacity ( $\text{mg}\cdot\text{dm}^{-3}$ ) $v$ = linear flow speed ( $\text{dm}\cdot\text{min}^{-1}$ ) $L$ = bed depth (dm) $C_0$ = initial concentration of contaminant ( $\text{mg}\cdot\text{dm}^{-3}$ ) $C$ = concentration of the effluent ( $\text{mg}\cdot\text{dm}^{-3}$ ) $t$ = residence time of the solution in the column (min)
Thomas (Th)	$\frac{C}{C_0} = \frac{1}{1 + \exp\left[\frac{K_{Th}}{Q}(q_0X - C_0V)\right]}$	$K_{Th}$ = Thomas' constant ( $\text{cm}^3(\text{mg}\cdot\text{min})^{-1}$ ) $q_0$ = maximum concentration of solute in the solid phase ( $\text{mg}\cdot\text{g}^{-1}$ ) $X$ = amount of adsorbent in the column (g) $Q$ = flow speed ( $\text{cm}^3\cdot\text{min}^{-1}$ ) $V$ = volume of the effluent at the time of operation ( $\text{dm}^3$ )
Yoon–Nelson (YN)	$\frac{C}{C_0} = \frac{\exp(K_{YN}t - \tau K_{YN})}{1 + \exp(K_{YN}t - \tau K_{YN})}$	$K_{YN}$ = Yoon–Nelson proportionality constant ( $\text{min}^{-1}$ ) $\tau$ = time required to retain 50% of the initial adsorbate (min)
Dose–Response (DR)	$\frac{C}{C_0} = 1 - \frac{1}{1 + \left(\frac{C_0Q}{q_0X}\right)^a}$	$a$ = model constant $q_0$ = adsorption capacity of the adsorbent ( $\text{mg}\cdot\text{g}^{-1}$ ) $X$ = amount of adsorbent in the column (g) $Q_t$ = flow rate ( $\text{cm}^3\cdot\text{min}^{-1}$ )

Source: adapted from ARIM *et al.* [2018].

The adjustment of parameters to the break curve models was obtained by non-linear regression. The experimental capacity of the column for each breakage curve was determined using Equation (2).

$$Q_{\text{tot}} = \frac{Q}{1000m} \int_0^{ts} C_t - C_0 dt \quad (2)$$

where:  $Q_{\text{tot}}$  = concentration of Cr(VI) ion in the adsorbent ( $\text{mg}\cdot\text{g}^{-1}$ );  $C_0$  = concentration of the ion or ions in the feed-in aqueous solution;  $C_t$  = output concentration of the ions studied in the aqueous solution ( $\text{mg}\cdot\text{dm}^{-3}$ );  $ts$  = time taken for the cake to convert the initial concentration of the ion studied into the final concentration (min);  $Q$  = flow rate ( $\text{cm}^3\cdot\text{min}^{-1}$ );  $m$  = mass of the cake packed in the column (g).

## RESULTS

### CHARACTERISATION OF THE BIO-ADSORBENT

Scanning Electron Microscopy (SEM) microphotographs and Energy Dispersive X-ray (EDS) spectra of the yam shell before and after chromium(VI) adsorption are shown in Figure 1. After

the adsorption process, the metal ion coverage of the bio-adsorbent pores is observed [KUPPUSAMY *et al.* 2016].

Table 3 summarises the composition of yam shells before and after the Cr(VI) adsorption from EDS. The EDS spectrum showed that yam shells have diverse structure rich in carbon (47.40% w/w), oxygen (43.20% w/w), and potassium (4.46% w/w). Moreover, the study discovered traces of such elements as silicon, aluminium, phosphorus, and iron, which can be related to functional groups present in lignocellulosic materials (cellulose,

hemicellulose, lignin, and pectin) [CORRAL-ESCÁRCEGA *et al.* 2017]. The adsorbent has the ability to capture cations due to electrostatic forces, and white particles are observed on micrographs [DENG *et al.* 2020]. After the adsorption, it is presented in the EDS, with the creation of the characteristic peak of Cr(VI) in 1, 5.6, and 5.8 keV, as well as the decrease of the % in weight of elements such as O, Si, K, and Fe, which could be explained by the interaction of these elements with metallic ions in active centres of the bio-adsorbent through ion exchange. This promotes the formation of micro-complexes and precipitation [MEDELLIN-CASTILLO *et al.* 2017].

### ADSORPTION TESTS

After conducting the Cr(VI) adsorption test on yam peels, the effect of temperature, particle size, and adsorbent dose on the process was evaluated. The metal removal efficiency was calculated using Equation (1). The tests were conducted at a constant flow rate of  $0.75 \text{ cm}^3\cdot\text{s}^{-1}$  with an initial contaminant concentration of  $100 \text{ mg}\cdot\text{dm}^{-3}$ . The results are summarised in Figures 2, 3, and 4. A maximum removal rate of 98.3% was obtained. This result found that the best condition for removing chromium(VI) was 0.355 of particle size,  $55^\circ\text{C}$ , and 89 mm of bed height.

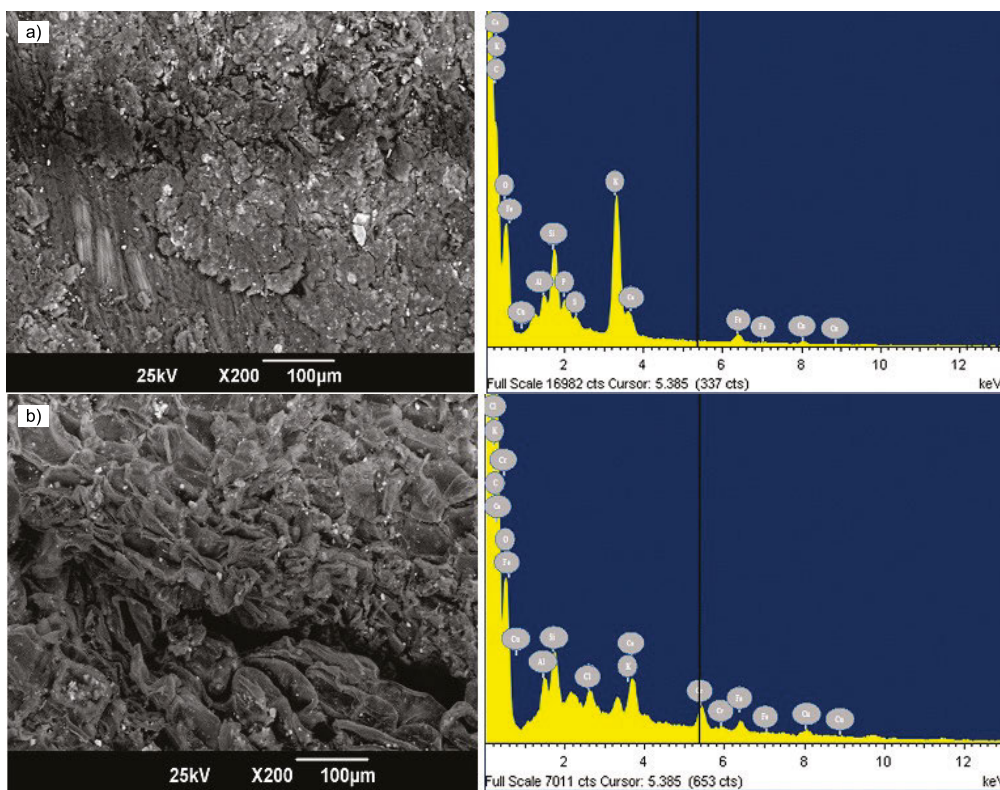


Fig. 1. Scanning Electron Microscopy micrographs of yam peels: a) before, b) after Cr(VI) adsorption; source: own study

Table 3. Composition of yam shells before and after adsorption of Cr(VI)

Yam			Yam-Cr(VI)		
element	weight (%)	atomic (%)	element	weight (%)	atomic (%)
C	47.40	57.07	C	54.50	63.25
O	43.20	39.05	O	39.67	34.56
Al	0.75	0.40	Al	0.82	0.42
Si	2.16	1.11	Si	1.21	0.60
P	0.66	0.31	Cl	0.45	0.18
S	0.17	0.08	K	0.44	0.16
K	4.46	1.65	Ca	0.99	0.34
Ca	0.34	0.12	Cr	0.88	0.24
Fe	0.60	0.16	Fe	0.59	0.15
Cu	0.27	0.06	Cu	0.45	0.10
<b>Total</b>	<b>100.00</b>	<b>100.00</b>	<b>Total</b>	<b>100.00</b>	<b>100.00</b>

Source: own study.

The results show that biomass is very effective at adsorbing Cr(VI) ions on its surface due to functional groups involved in ion exchange with the contaminant due to its lignocellulosic nature and porous structure. It has been previously reported that the yam shell is rich in cellulose and hemicellulose, compounds that have in their structure multiple hydroxyl, carboxyl and carbonyl groups, which behave as active centres and influence the process of heavy metal removal [KUPPUSAMY *et al.* 2016].

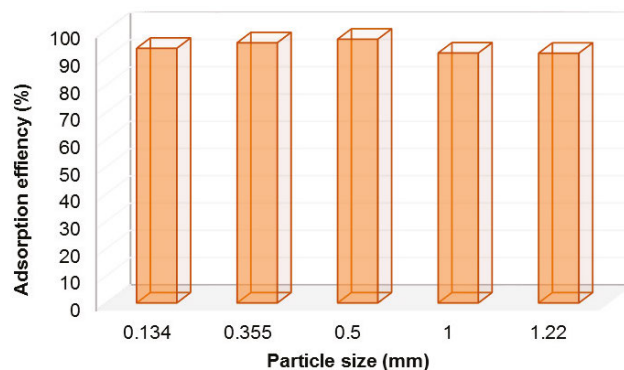


Fig. 2. Particle size effect; source: own study

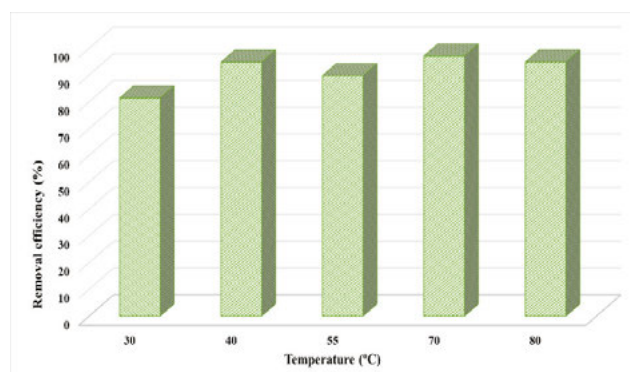


Fig. 3. Effect of temperature; source: own study

The selectivity of the yam shell for Cr(VI) at the temperature, bed height, and particle size evaluated can be explained as a function of the ionic radius of 0.69, which benefits the diffusion of the metal in a solution and at active sites

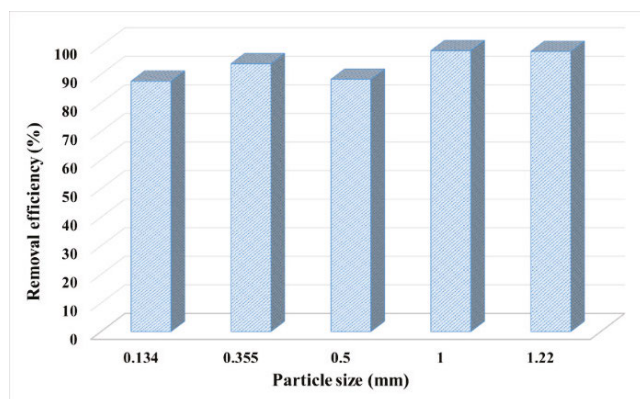


Fig. 4. Effect of bed height; source: own study

[RANASINGHE *et al.* 2018]. Particle size is a highly influential parameter in adsorption studies because a smaller particle size implies a larger adsorption area [PENG *et al.* 2018]. The present study found that a decreasing particle size increased removal efficiency. As for the temperature, it is possible to observe that it is directly proportional, which indicates that with the increase in temperature, a percentage of adsorption gets higher due to the proportional increase of the speed of ions in the solution with temperature. This increases the diffusion from the solution towards the exposed surface of the adsorbent [AKPOMIE *et al.* 2018]. However, the effect of this variable can be considered negligible due to the excellent performance of biomass. This indicates that energy changes at temperature values evaluated on the system and does not have a significant effect on the removal and transfer of mass. On the other hand, the increase of the bed height also favours the removal efficiency. Due to the increase of the adsorbent dose, there are many union sites for adsorption [HAROOON *et al.* 2016].

The analysis of variance (ANOVA) performed in Statgraphics Centurion XVII is shown in Table 4. The bed height and particle size have a significant statistical influence on the interaction between the Cr(VI) ion and the active centres of the adsorbent since the *P*-value is less than 0.05. This statistical significance is there since the higher the bed height and particle size, the more adsorption centres will be formed due to the amount of bio-adsorbent available and the increase of the exposed surface area when the particle diameter is lower [MALKOC, NUHOGLU 2006].

#### MODELLING OF THE BREAKAGE CURVE

The breakage curve is made to evaluate the bed saturation time. It is usually expressed in terms of concentration, that is, as the ratio between the metal concentration in the liquid at the exit and the entrance to the column ( $C/C_0$ ) [ABDOLALI *et al.* 2017]. The Cr(VI) adsorption breakdown curve on yam shells was evaluated at the best condition found: 0.355 particle size, 55°C, and 89 mm bed height, with a flow rate of 0.75 cm<sup>3</sup>·min<sup>-1</sup> and initial concentration of 100 mg·dm<sup>-3</sup>, for five hours. The experimental data were adjusted to the Adams–Bohart, Thomas, Yoon–Nelson, and Dose–Response models (Fig. 5).

From Equation (2), the adsorption capacity of the bed was calculated at 61.75 mg·g<sup>-1</sup>; this was attributed to the abundance of functional groups due to the lignocellulosic adsorbent composition. The result obtained in the present study is superior to that

Table 4. Analysis of variance (ANOVA) for chromium(VI) adsorption

Source	Sum of squares	DF	Ratio-F	P-value
A: particle size	18.677	1	10.25	0.0493
B: temperature	11.6099	1	6.37	0.0858
C: bed height	34.9056	1	19.16	0.0221
AA	2.52179	1	1.38	0.3242
AB	0.646872	1	0.36	0.5932
AC	1.2482	1	0.69	0.4685
BB	3.21756	1	1.77	0.2759
BC	0.34019	1	0.19	0.6948
CC	11.8487	1	6.50	0.0839
Total error	5.46544	3		
Total (corr.)	161.657	12		

Explanation: DF = degrees of freedom.

Source: own study.

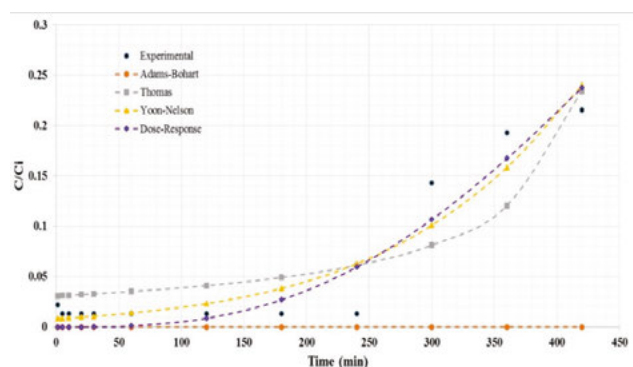


Fig. 5. Adjustment to breakage curve models of Cr(VI) adsorption data to Adams–Bohart, Thomas, Yoon–Nelson and Dose–Response models; source: own elaboration

reported by RUIZ-PATERNINA *et al.* [2019]. The application of yam, banana, and palm bagasse residues achieved an adsorption capacity for Cr(VI) of 28.01, 18.25, and 49.58 mg·g<sup>-1</sup>. The adsorption capacity of 29.85 mg·g<sup>-1</sup> was obtained [VILLABONA-ORTIZ *et al.* 2020]. The breakdown curve made for Cr(VI) adsorption shows that the highest removal of the metal ion occurs in the first moments of contact with the bio-adsorbent. It also indicates a breakpoint close to 360 min, showing a trend in decreasing adsorption capacity due to the gradual occupation of active sites available [RANGABHASHIYAM *et al.* 2016]. However, the balance is not reached, so it is established that the yam shell has a high capacity of Cr(VI) adsorption, so its use is recommended [MISHRA *et al.* 2016].

Based on Figure 5 and the data shown in Table 5, it can be concluded that models that best describe the adsorption breakdown curve of Cr(VI) on yam shells are Dose–Response and Yoon–Nelson with  $R^2$  of 0.96 and 0.95, respectively. The theoretical value of maximum bed adsorption capacity calculated by the model is close to the experimental one, which shows the excellent fit of the Dose–Response model [BLANES *et al.* 2016].

**Table 5.** Adjustment parameters of the breaking curve models

Model	Parameter	Value
Thomas	$K_{Th}$ ( $\text{cm}^3 (\text{mg}\cdot\text{min})^{-1}$ )	0.6718
	$q_{Th}$ ( $\text{mg}\cdot\text{g}^{-1}$ )	15.6667
	SS	0.0016
	$R^2$	0.8924
Dose-Response	$q_{DR}$ ( $\text{mg}\cdot\text{g}^{-1}$ )	62.1776
	$a$	0.6725
	SS	0.0006
	$R^2$	0.9582
Yoon-Nelson	$K_{YN}$ ( $\text{min}^{-1}$ )	0.0086
	$\tau$ (min)	533.6739
	SS	0.0007
	$R^2$	0.9468
Adams-Bohart	$K_{AB}$ ( $\text{dm}^3\cdot(\text{mg}\cdot\text{min})^{-1}$ )	5368.71
	$N_0$ ( $\text{mg}\cdot\text{dm}^{-3}$ )	154654.57
	SS	0.01
	$R^2$	0.0

Explanations:  $K_{Th}$  = Thomas' speed constant,  $q_{Th}$  = maximum concentration of solute in the solid phase, SS = sum of squares,  $R^2$  = coefficient of correlation,  $q_{D-R}$  = maximum solute concentration in the solid phase,  $a$  = Dose-Response model constant,  $K_{Y-N}$  = Yoon-Nelson's constant of proportionality,  $\tau$  = time required to retain 50% of the initial adsorbate,  $K_{A-B}$  = Adams-Bohart's constant of proportionality,  $N_0$  = maximum volumetric sorption capacity,  $R^2$  = determination coefficient.

Source: own study.

However, it is difficult to relate the empirical parameter “ $a$ ” to the experimental conditions studied in this system, making it difficult to scale the system with this model [VERA *et al.* 2019]. On the other hand, the adjustment of the Yoon-Nelson's model suggests that the mechanism of adsorption is of the Langmuir type, followed by chemical adsorption of pseudo-second-order, which is evident in the precipitations and formation of micro-complexes evidenced in the SEM micrographs reported in Figure 1 [SRIVASTAVA *et al.* 2019]. The fit of the break curve to the Yoon-Nelson and Dose-Response models has been previously reported using epichlorohydrin and N, N-dimethylformamide modified corn-stalks as adsorbents [CHEN *et al.* 2012], mountain oak [MALKOC *et al.* 2006], olive stone [MARTÍN-LARA *et al.* 2017], and *Quercus crassipes* [ARANDA-GARCÍA, CRISTIANI-URBINA 2020].

## CONCLUSIONS

1. The removal efficiency of Cr(VI) was between 92.4 and 98.3%, which shows the affinity of the yam shell for the ion.
2. The Scanning Electron Microscopy (SEM) and Energy Dispersive X-ray (EDS) analysis of yam shells showed a heterogeneous, porous structure, with functional groups, such as hydroxyl, carboxyl, carbonyl, and amines, characteristic of lignocellulosic materials.

3. It was found that the increase of the bed height and the decrease of the particle size positively impact the process. The maximum capacity of adsorption was obtained in the bed of  $61.75 \text{ mg}\cdot\text{g}^{-1}$  with a break time of 360 min, at the best conditions found: 0.355 of particle size,  $55^\circ\text{C}$ , and 89 mm of bed height.
4. The Yoon-Nelson and Dose-Response models adjusted the experimental data of the  $R^2$  breaking curve by 0.95 and 0.96, respectively.
5. Based on the results obtained, the bio-adsorbent evaluated is recommended to remove Cr(VI) in an aqueous solution in a continuous system.

## ACKNOWLEDGEMENTS

The authors thank the University of Cartagena for supporting the development of this research in terms of laboratories, software, and researchers' time.

## REFERENCES

- ABDOLALI A., NGO H.H., GUO W., ZHOU J.L., ZHANG J., LIANG S., CHANG S. W., NGUYEN D.D., LIU Y. 2017. Application of a breakthrough biosorbent for removing heavy metals from synthetic and real wastewaters in a lab-scale continuous fixed-bed column. *Bioresource Technology*. Vol. 229 p. 78–87. DOI 10.1016/j.biortech.2017.01.016.
- ACHMAD R.T., BUDIAWAN, AUERKARI E.I. 2017. Effects of chromium on human body. *Annual Research and Review in Biology*. Vol. 13(2) p. 1–8. DOI 10.9734/ARRB/2017/33462.
- AKPOMIE K.G., ELUKE L.O., AJIWE V.I., ONYEMEZIRI A.C. 2018. Attenuation kinetics and desorption performance of *Artocarpus altilis* seed husk for Co(II), Pb(II) and Zn(II) ions. *Iranian Journal of Chemistry and Chemical Engineering*. Vol. 37(3) p. 171–186.
- ARANDA-GARCÍA E., CRISTIANI-URBINA E. 2020. Hexavalent chromium removal and total chromium biosorption from aqueous solution by *Quercus crassipes* acorn shell in a continuous up-flow fixed-bed column: Influencing parameters, kinetics, and mechanism. *PLOS ONE*. Vol. 15(1), e0227653. DOI 10.1371/journal.pone.0227953.
- ARIM A.L., NEVES K., QUINA M.J., GANDO-FERREIRA L.G. 2018. Experimental and mathematical modelling of Cr(III) sorption in fixed-bed column using modified pine bark. *Journal of Cleaner Production*. Vol. 183 p. 272–281. DOI 10.1016/j.jclepro.2018.02.094.
- BHANVASE B.A., UGWEKAR R.P., MARKAR R.B. 2017. *Novel water treatment and separation methods: Simulation of chemical processes*. Waretown. Apple Academic Press Inc. ISBN 9781774636503 pp. 356.
- BHARATHI K.S., RAMESH S.K.P.T. 2013. Fixed-bed column studies on biosorption of crystal violet from aqueous solution by *Citrullus lanatus* rind and *Cyperus rotundus*. *Applied Water Science*. Vol. 3 p. 673–687. DOI 10.1007/s13201-013-0103-4.
- BIBAJ E., LYSIGAKI K., NOLAN J.W., SEYEDSALEHI M., DELIYANNI E.A., MITROPOULOS A.C., KYZAS G.Z. 2019. Activated carbons from banana peels for the removal of nickel ions. *International Journal of Environmental Science and Technology*. Vol. 16(2) p. 667–680. DOI 10.1007/s13762-018-1676-0.

- BLANES P.S., BORDONI M.E., GONZÁLEZ J.C., GARCÍA S.I., ATRIA A.M., SALA L.F., BELLU S.E. 2016. Application of soy hull biomass in removal of Cr(VI) from contaminated waters. kinetic, thermodynamic and continuous sorption studies. *Journal of Environmental Chemical Engineering*. Vol. 4(1) p. 516–526. DOI 10.1016/j.jece.2015.12.008.
- CHEN S., YUE Q., GAO B., LI Q., XU X., FU K. 2012. Adsorption of hexavalent chromium from aqueous solution by modified corn stalk: A fixed-bed column study. *Bioresource Technology*. Vol. 113 p. 114–120. DOI 10.1016/j.biortech.2011.11.110.
- CHERDCHOO W., NITHETHAM S., CHAROENPANICH J. 2019. Removal of Cr(VI) from synthetic wastewater by adsorption onto coffee ground and mixed waste tea. *Chemosphere*. Vol. 221 p. 758–767. DOI 10.1016/j.chemosphere.2019.01.100.
- CHINYELU I.E., ODEBEATU C.C., OBUMSELU O.F., ILOAMAEKE I.M.J., KAMMEJE T.J. 2018. Isotherm studies of adsorption of Cr(VI) ions onto coconut husk. *International Journal of Biochemistry, Biophysics & Molecular Biology*. Vol. 3(2) p. 38–44. DOI 10.11648/j.ijbbmb.20180302.13.
- CORRAL-ESCARCEGA M.C., RUIZ-GUTIÉRREZ M.G., QUINTERO-RAMOS A., MELÉNDEZ-PIZARRO C.O., LARDIZABAL-GUTIÉRREZ D., CAMPOS-VEÑEGAS K. 2017. Use of biomass-derived from pecan nut husks (*Carya illinoensis*) for chromium removal from aqueous solutions. Column modeling and adsorption kinetics studies. *Revista Mexicana de Ingeniería Química*. Vol. 16(3) p. 939–953.
- DEMIREL M., KAYAN B. 2012. Application of response surface methodology and central composite design for the optimization of textile dye degradation by wet air oxidation. *International Journal of Industrial Chemistry*. Vol. 3(1) p. 1–10. DOI 10.1186/2228-5547-3-24.
- DENG Y., HUANG S., DONG C., MENG Z., WANG X. 2020. Competitive adsorption behaviour and mechanisms of cadmium, nickel and ammonium from aqueous solution by fresh and ageing rice straw biochars. *Bioresource Technology*. Vol. 303, 122853. DOI 10.1016/j.biortech.2020.122853.
- ELABBAS S., OUZZANI N., MANDI L., BERREKHIS F., PERDICAKIS M., PONTVIANNE S., PONS M.N., LAPICQUE F., LECLERC J.P. 2016. Treatment of highly concentrated tannery wastewater using electrocoagulation: Influence of the quality of aluminium used for the electrode. *Journal of Hazardous Materials*. Vol. 319 p. 69–77. DOI 10.1016/j.jhazmat.2015.12.067.
- HAROON H., ASHFAQ T., HUSSAIN GARDAZI S.M., SHERAZI T.A., ALI M., RASHID N., BILAL M. 2016. Equilibrium kinetic and thermodynamic studies of Cr(VI) adsorption onto a novel adsorbent of *Eucalyptus camaldulensis* waste: Batch and column reactors. *Korean Journal of Chemical Engineering*. Vol. 33(10) p. 2898–2907. DOI 10.1007/s11814-016-0160-0.
- JAFARI S.A., JAMALI A. 2016. Continuous cadmium removal from aqueous solutions by seaweed in a packed-bed column under consecutive sorption-desorption cycles. *Korean Journal of Chemical Engineering*. Vol. 33(4) p. 1296–1304. DOI 10.1007/s11814-015-0261-1.
- KUPPUSAMY S., PALANISAMI T., LEE Y.B., NAIDU R. 2016. Oak (*Quercus robur*) acorn peel as a low-cost adsorbent for hexavalent chromium removal from aquatic ecosystems and industrial effluents. *Water, Air, & Soil Pollution*. Vol. 227, 62. DOI 10.1007/s11270-016-2760-z.
- MALKOC E., YASAR N. 2006. Fixed bed studies for the sorption of chromium(VI) onto tea factory waste. *Chemical Engineering Science*. Vol. 61(13) p. 4363–4372. DOI 10.1016/j.ces.2006.02.005.
- MALKOC E., NUHOGLU Y., ABALI Y. 2006. Cr(VI) adsorption by waste acorn of *Quercus ithaburensis* in fixed beds: Prediction of breakthrough curves. *Chemical Engineering Journal*. Vol. 119(1) p. 61–68. DOI 10.1016/j.cej.2006.01.019.
- MARTÍN-LARA M.Á., TRUJILLO MIRANDA M.C., RONDA GÁLVEZ A., PÉREZ MUÑOZ A., CALERO DE HOCES M. 2017. Valorization of olive stone as adsorbent of chromium(VI): Comparison between laboratory- and pilot-scale fixed-bed columns. *International Journal of Environmental Science and Technology*. Vol. 14(12) p. 2661–2674. DOI 10.1007/s13762-017-1345-8.
- MEDELLIN-CASTILLO N., HERNÁNDEZ-RAMÍREZ M.G., SALAZAR-RÁBAGO J.J., LABRADA-DELGADO G.J., ARAGÓN-PIÑA A. 2017. Bioadsorción de plomo (II) presente en solución acuosa sobre residuos de fibras naturales procedentes de la industria ixtlera (*Agave lechuguilla* Torr. y *Yucca carnerosana* (Trel.) McKelvey) [Biosorption of lead (II) in aqueous solution onto residues of natural fibers from the ixtlera industry (*Agave lechuguilla* Torr. and *Yucca carnerosana* (Trel.) McKelvey)]. *Revista Internacional de Contaminación Ambiental*. Vol. 33(2) p. 269–280. DOI 10.20937/RICA.2017.33.02.08.
- MISHRA A., TRIPATHI B.D., RAI A.K. 2016. Packed-bed column biosorption of chromium(VI) and nickel(II) onto Fenton modified *Hydrilla verticillata* dried biomass. *Ecotoxicology and Environmental Safety*. Vol. 132 p. 420–428. DOI 10.1016/j.ecoenv.2016.06.026.
- PARLAYICI Ş., PEHLIVAN E. 2019. Comparative study of Cr(VI) removal by bio-waste adsorbents: Equilibrium, kinetics, and thermodynamic. *Journal of Analytical Science and Technology*. Vol. 10(1), 15. DOI 10.1186/s40543-019-0175-3.
- PENG S.H., WANG R., YANG L.Z., HE L., HE X., LIU X. 2018. Biosorption of copper, zinc, cadmium and chromium ions from aqueous solution by natural foxtail millet shell. *Ecotoxicology and Environmental Safety*. Vol. 165 p. 61–69. DOI 10.1016/j.ecoenv.2018.08.084.
- RANASINGHE S.H., NAVARATNE A.N., PRIYANTHA N. 2018. Enhancement of adsorption characteristics of Cr(III) and Ni(II) by surface modification of jackfruit peel biosorbent. *Journal of Environmental Chemical Engineering*. Vol. 6(5) p. 5670–5682. DOI 10.1016/j.jece.2018.08.058.
- RANGABHASHIYAM S., GIRI NANDAGOPAL M.S., NAKKEERAN E., SELVARAJU N. 2016. Adsorption of hexavalent chromium from synthetic and electroplating effluent on chemically modified *Swietenia mahagoni* shell in a packed bed column. *Environmental Monitoring and Assessment*. Vol. 188(7) p. 1–13. DOI 10.1007/s10661-016-5415-z.
- RODRIGUES E., ALMEIDA O., BRASIL H., MORAES D., DOS REIS M.A.L. 2019. Applied clay science adsorption of chromium (VI) on hydro-talcite-hydroxyapatite material doped with carbon nanotubes: Equilibrium, kinetic and thermodynamic study. *Applied Clay Science*. Vol. 172 p. 57–64. DOI 10.1016/j.clay.2019.02.018.
- RONDA A., MARTÍN-LARA M.A., ALMENDROS A.I., PÉREZ A., BLÁZQUEZ G. 2015. Comparison of two models for the biosorption of Pb(II) using untreated and chemically treated olive stone: Experimental design methodology and Adaptive Neural Fuzzy Inference System (ANFIS). *Journal of the Taiwan Institute of Chemical Engineers*. Vol. 54 p. 45–56. DOI 10.1016/j.jtice.2015.03.004.
- RUIZ-PATERNINA E.B., VILLABONA-ORTIZ Á., TEJADA-TOVAR C., ORTEGA-TORO R. 2019. Estudio termodinámico de la remoción de níquel y cromo en solución acuosa usando adsorbentes de origen agroindustrial [Thermodynamic study of the removal of nickel and chromium in aqueous solution using adsorbents of agro-industrial origin]. *Información Tecnológica*. Vol. 30(6) p. 3–10. DOI 10.4067/S0718-07642019000600003.
- SAHU O., SINGH N. 2019. Significance of bioadsorption process on textile industry wastewater. In: *The impact and prospects of green*

- chemistry for textile technology. Eds. Shahid-ul-Islam, B.S. Butola. The Textile Institute Book Series. Vol. 13 p. 367–416. DOI 10.1016/B978-0-08-102491-1.00013-7.
- SRIVASTAVA S., AGRAWAL S.B., MONDAL M.K. 2019. Fixed bed column adsorption of Cr(VI) from aqueous solution using nanosorbents derived from magnetite impregnated *Phaseolus vulgaris* Husk. Environmental Progress and Sustainable Energy. Vol. 38(s1) p. S68–S76. DOI 10.1002/ep.12918.
- SUKUMAR C., JANAKI V., VIJAYARAGHAVAN K., KAMALA-KANNAN S., SHANTHI K. 2017. Removal of Cr(VI) using co-immobilized activated carbon and *Bacillus subtilis*: Fixed-bed column study. Clean Technologies and Environmental Policy. Vol. 19(1) p. 251–258. DOI 10.1007/s10098-016-1203-2.
- VERA L.M., BERMEJO D., UGUÑA M.F., GARCIA N., FLORES M., GONZÁLEZ E. 2019. Fixed bed column modeling of lead(II) and cadmium(II) ions biosorption on sugarcane bagasse. Environmental Engineering Research. Vol. 24(1) p. 31–37. DOI 10.4491/eer.2018.042.
- VILLABONA-ORTIZ Á., TEJADA-TOVAR C., RUIZ-PATERNINA E., FRIAS-GONZÁLEZ J.D., BLANCO-GARCÍA G.D. 2020. Optimization of the effect of temperature and bed height on Cr (VI) bioadsorption in continuous system. Revista Facultad de Ingeniería. Vol. 29(54), e10477. DOI 10.19053/01211129.v29.n54.2020.10477.